Adjustable subwavelength localization in a hybrid plasmonic waveguide

S. Belan,[1,2,*] **S. Vergeles,**[1,2] **P. Vorobev**[1,2]

[1]*Landau Institute for Theoretical Physics RAS,*
Kosygina 2, 119334, Moscow, Russia
[2]*Moscow Institute of Physics and Technology,*
Dolgoprudnyj, Institutskij per. 9, 141700, Moscow Region, Russia

[*]*sergb27@yandex.ru*

Abstract: The hybrid plasmonic waveguide consists of a high-permittivity dielectric nanofiber embedded in a low-permittivity dielectric near a metal surface. This architecture is considered as one of the most perspective candidates for long-range subwavelength guiding. We present qualitative analysis and numerical results which reveal advantages of the special waveguide design when dielectric constant of the cylinder is greater than the absolute value of the dielectric constant of the metal. In this case the arbitrary subwavelength mode size can be achieved by controlling the gap width. Our qualitative analysis is based on consideration of sandwich-like conductor-gap-dielectric system. The numerical solution is obtained by expansion of the hybrid plasmonic mode over single cylinder modes and the surface plasmon-polariton modes of the metal screen and matching the boundary conditions.

© 2013 Optical Society of America

OCIS codes: (130.0130) Integrated optics; (240.6680) Surface plasmons; (230.7370) Waveguides.

References and links

1. M. Born, E. Wolf, *Principles of Optics* (Cambridge Univ. Press, 1999).
2. D. K. Gramotnev and S. I. Bozhevolnyi, "Plasmonics beyond the diffraction limit," Nat. Phot. **4**, 83-91 (2010).
3. R. F. Oulton , V. J. Sorger, D. A. Genov, D. F. P. Pile, and X. Zhang, "Hybrid plasmonic waveguide for subwavelength confinement and long-range propagation," Nat. Phot. **2**(8), 496-500 (2008).
4. V. J. Sorger, Z. Ye, R. F. Oulton, Y. W. G. Bartal, X. Yin, and X. Zhang, "Experimental demonstration of low-loss optical waveguiding at deep sub-wavelength scales," Nat. Commun. **2**, 331 (2011).
5. I. Avrutsky, R. Soref, and W. Buchwald, "Sub-wavelength plasmonic modes in a conductor-gap-dielectric system with a nanoscale gap," Opt. Express **18**(1), 348-363 (2010).
6. R. Borghi, F. Gori, M. Santarsiero, F. Frezza, and G. Schettini, "Plane-wave scattering by a perfectly conducting circular cylinder near a plane surface: cylindrical-wave approach," J. Opt. Soc. Am. A. **13**(3), 483-493 (1996).
7. R. Borghi, M. Santarsiero, F. Frezza, and G. Schettini, "Plane-wave scattering by a dielectric circular cylinder parallel to a general reflecting flat surface," J. Opt. Soc. Am. A. **14**(7), 1500-1504 (1997).
8. J. Takahara, S. Yamagishi, H. Taki, A. Morimoto, and T. Kobayashi, "Guiding of a one-dimensional optical beam with nanometer diameter," Opt. Lett. **82**(8), 1158-1160 (1997).
9. I. Avrutsky, I. Salakhutdinov, J. Elser, and V. Podolskiy, "Highly confined optical modes in nanoscale metaldielectric multilayers," Phys. Rev. B **75**(24), 241402 (2007).
10. A. Ishikawa, S. Zhang, D. A. Genov, G. Bartal, and X. Zhang, "Deep Subwavelength Terahertz Waveguides Using Gap Magnetic Plasmon", Phys. Rev. Let. **102**, 043904 (2009).
11. S. H. Nam, A. J. Taylor, and A. Efimov, "Subwavelength hybrid terahertz waveguides," Opt. Express. **17**(25), 22890-22897 (2009).
12. P. R. West, S. Ishii, G. V. Naik, N. K. Emani, V. M. Shalaev, and A. Boltasseva, "Searching for better plasmonic materials," Laser Photonics Rev. **4**, 795-808 (2010).

13. D. Marcuse, *Light Transmission Optics* (New York: Van Nostrand Reinhold, 1972).
14. A. G. Bulushev, E. M. Dianov, and O. G. Okhotnikov, "Propagation of the radiation in two identical coupled waveguides," Quantum Electron. **15**, 1433-1441 (1988).
15. W. Zakowicz, "Two coupled dielectric cylindrical waveguides," J. Opt. Soc. Am. A **14**(3), 580-587 (1997).
16. R. F. Oulton, V. J. Sorger, T. Zentgraf, Ren-Min Ma, C. Gladden, L. Dai, G. Bartal, and X. Zhang, "Plasmon lasers at deep subwavelength scale," Nature **461**, 629-632 (2009).
17. I. Avrutsky, "Surface plasmons at nanoscale relief gratings between a metal and a dielectric medium with optical gain," Phys. Rev. B **70**, 155416 (2004).
18. R. Borghi, F. Frezza, M. Santarsiero, and G. Schettini, "Angular spectrum of modified cylindrical wave-functions," Int. J. Infrared Millim. Waves **20**(10), 1795-1801 (1999).

1. Introduction

The creation of the waveguides capable of guiding light with deep subwavelength confinement is of great interest for practical applications. These devices may throw open the doors to nanoscale optical communications, quantum computing, nanoscale lasers and bio-medical sensing. The main problem on the way to practical realization is the diffraction limit of light in dielectric media. Electromagnetic energy cannot be localized into nanoscale region much smaller than the wavelength of light in the dielectric [1]. The possible solution to this problem is using of the materials with negative dielectric permittivity. For example, metals are known to exhibit this property below the plasma frequency. Metal structures provide guiding of the surface plasmon-polaritons (SPP), which can be strongly localized near metal-dielectric interfaces [2]. However the propagation length of the strongly confined plasmonic modes is not large enough due to the presence of Ohmic losses in the dissipative metal regions.

The new approach for this challenge integrates dielectric waveguide with plasmonic one. The hybrid plasmonic waveguide consists of a high-permittivity dielectric nanofiber separated from a metal screen by low-permittivity dielectric nanoscale gap [3]. Both the single fiber and the silver-dielectric interface cannot provide strong mode confinement at optical and near infrared frequencies, but such hybrid conductor-gap-dielectric architecture has experimentally demonstrated deep subwavelength optical waveguiding [4]. Relatively large propagation distance has been achieved due to low loss tangent $tg = \varepsilon''_m / \varepsilon'_m$ at the operating frequency and the specific spatial structure of the guiding mode with field confinement within non dissipative gap region.

In the present paper we show that the hybrid plasmon polariton (HPP) mode confinement can be considerably risen by a specific choice of the materials, when the dielectric constant of the cylinder is greater than the absolute value of the dielectric constant of the metal screen. The main advantage of the choice is the hyperbolic-like dependence of the effective index on the gap width. This feature allows to achieve arbitrary subwavelength mode size at any frequency by tuning the distance between the cylinder and the metal. To justify our approach we theoretically investigate propagation of the HPP-mode. First we give qualitative analysis basing on the consideration of plane sandwich-like conductor-gap-dielectric waveguide structure (CGD) [5]. We derive exact analytical expression for effective index of the fundamental CGD-mode and give criterion when the HPP-mode is CGD-like. Finally, we present semi-analytical approach for describing of the HPP-mode propagation. Similar approach has been previously applied for plane wave scattering by a cylinder placed near the plane surface [6, 7].

The scheme is based on expansion of the HPP-mode over single cylinder modes and the surface plasmon polariton modes of the metal-dielectric interface and matching the boundary conditions for electromagnetic field components. Numerically obtained dispersion relations confirm the advantages of our design of the hybrid waveguide. The results were verified by means of the finite element method (FEM) using COMSOL.
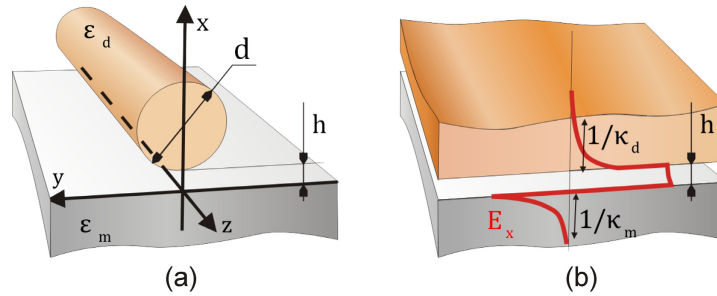
Fig. 1. **a)** Geometry of the waveguide; **b)** Plain waveguide with the same width of the gap.

2. Qualitative description

The geometry of the hybrid waveguide is the following: a circular dielectric cylinder of diameter d and permittivity ε_d is placed above a metal screen of permittivity ε_m. The width of the gap between the cylinder and the metal screen is h, see Fig. 1(a). Let us choose the Cartesian reference system as it is shown in Fig. 1: z-axis is directed along the waveguide, whereas x-axis is directed normally to the metal screen. We consider a plasmon-polariton mode of frequency ω and the propagation constant β propagating along z-axis. Thus, all electromagnetic field components depend on time and z-coordinate as $\exp[i\beta z - i\omega t]$. We assume, that responses of both dielectric and metal on electromagnetic field are described by dielectric constants, which are ε_m and ε_d respectively. Generally, the outer medium may be not vacuum, but some dielectric medium having dielectric constant being equal to ε_g. All the materials are assumed to be nonmagnetic. To describe the mode confinement, it is convenient to introduce effective refractive index n_{eff}, which is defined as $n_{\text{eff}} = \beta/k$, where $k = \omega/c$ in the wavenumber in vacuum. The effective index determines the field penetration depth into the material with permittivity ε as $1/k\sqrt{n_{\text{eff}}^2 - \varepsilon}$. The penetration depth of the bound mode should be real in the unbounded waveguide constituents (metal and outer dielectric space), and may be imaginary for bounded constituents (fiber). The greater n_{eff} is the stronger degree of confinement.

Optimization for transversal field confinement implemented in paper [3] for hybrid waveguide shows that the thinner gaps provide higher localization. The fiber diameter is much greater than the the gap width in the case, and the mode is sufficiently localized in the region where the gap can be considered as approximately plain. In the region, the waveguide shape is close to plain sandwich like conductor-gap-dielectric (CGD) structure, see Fig. 1(b). The limit of plain CGD-model was considered in [5], where the properties of the bound fundamental mode were investigated. One of the main advantage of the CGD-mode is that effective index of the mode n_{CGD} is greater than the refractive index of the dielectric $\sqrt{\varepsilon_d}$, $n_{\text{CGD}} > \sqrt{\varepsilon_d}$. This implies, that the electromagnetic field of the mode decays exponentially into the dielectric cladding. Nevertheless, the analysis proposed in [5] is not applicable to HPP-mode of hybrid waveguide with optimal diameter found in [3]. The reason is that the mode of plain CGD-model indeed describes the HPP-mode only for large enough fiber diameter d otherwise HPP-mode should be considered as a result of hybridization of surface plasmon polariton modes and the modes of the single dielectric cylinder.

The main goal of the present work is to give the theoretical description of the hybrid waveguide and to find approaches to deeper localization of the HPP-mode. Comparative analysis of [3, 5] suggests, that in order to get stronger transversal miniaturization of the hybrid waveguide the CGD-like regime of propagation (with $n_{\text{eff}} > \sqrt{\varepsilon_d}$) should be achieved for the diameter
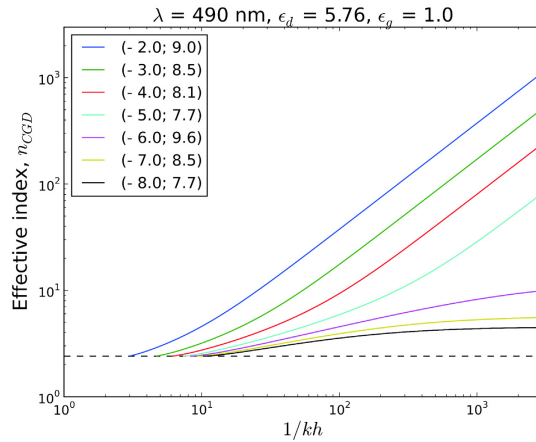
Fig. 2. Effective index n_{CGD} of the CGD-mode versus gap width h for different metal permittivity and critical gap width $(\varepsilon_m; h_c)$. The dielectric constants of the dielectric and gap region are $\varepsilon_d = 5.76$ and $\varepsilon_g = 1$ respectively at wavelength $\lambda = 490nm$.

which is much less than free space wavelength. Our analysis of the plain CGD-structure shows that the localization of the fundamental mode can be significantly risen for special set of materials, when absolute value of the metal dielectric constant is less than the dielectric constant of the dielectric cladding, $|\varepsilon_m| < \varepsilon_d$. For the case, the effective refractive index n_{CGD} is proportional to inverse width of the gap, $n_{\mathrm{CGD}} \propto 1/kh$, when the width h is small enough. To use the same effect for the hybrid waveguide, the cylinder diameter should sufficiently exceed some critical value d^*, which is determined by the condition that the transversal size of the plain part of the gap is comparable with the mode penetration depth into the dielectric $1/k\sqrt{n_{\mathrm{eff}}^2 - \varepsilon_d}$. The size of the plain part of the gap is evaluated as $2\sqrt{hd}$, thus the condition is $2\sqrt{hd^*} \approx 1/k\sqrt{n_{\mathrm{eff}}^2 - \varepsilon_d}$. For d greater enough than d^* the guiding mode can approach the strongly confined mode of the sandwich like system even if the diameter of the cylinder is much less than free space wavelength.

In order to give general physical argumentation of our results let us consider planar sandwich-like CGD-waveguide in detail. The wave vector of fundamental CGD-mode (which is TM-mode) can be calculated from equation [5]

$$\exp[2h\kappa_{\mathrm{g}}] = \frac{(\varepsilon_d \kappa_{\mathrm{g}} - \varepsilon_{\mathrm{g}}\kappa_d)(\varepsilon_m \kappa_{\mathrm{g}} - \varepsilon_{\mathrm{g}}\kappa_m)}{(\varepsilon_d \kappa_{\mathrm{g}} + \varepsilon_{\mathrm{g}}\kappa_d)(\varepsilon_m \kappa_{\mathrm{g}} + \varepsilon_{\mathrm{g}}\kappa_m)}, \tag{1}$$

where $\kappa_i = k\sqrt{n_{\mathrm{CGD}}^2 - \varepsilon_i}$ for each material, $i = m, g, d$ and n_{CGD} is the effective index of the mode. In particular, $1/\kappa_d$ and $1/\kappa_m$ are the penetration depths into the dielectric and the metal correspondingly. It is known that such plane three-layer waveguide supports the propagation of the bound eigen mode only if the width of the intermediate layer is less than some cut-off value h_c which is determined by the permittivities at given frequency

$$h_c = \frac{\lambda}{4\pi\sqrt{\varepsilon_d - \varepsilon_{\mathrm{g}}}} \log \frac{\varepsilon_m\sqrt{\varepsilon_d - \varepsilon_{\mathrm{g}}} - \varepsilon_{\mathrm{g}}\sqrt{\varepsilon_d - \varepsilon_m}}{\varepsilon_m\sqrt{\varepsilon_d - \varepsilon_{\mathrm{g}}} + \varepsilon_{\mathrm{g}}\sqrt{\varepsilon_d - \varepsilon_m}}. \tag{2}$$

When the thickness exceeds this critical value the fundamental CGD-mode becomes radiative with energy leaking into upper dielectric half space.
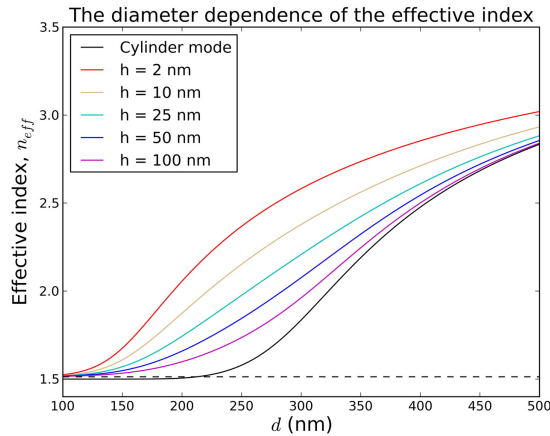
Fig. 3. Effective refractive index of the fundamental hybrid mode versus cylinder diameter d (coloured lines) compared with those of single fiber (black solid line) and SPP mode (lower black broken line). The upper black broken line corresponds to the refractive index of the cylinder. The dielectric constants of the cylinder, dielectric and metal are $\varepsilon_d = 12.25$ $\varepsilon_g = 2.25$ and $\varepsilon_m = -129 + 3.3i$ respectively at wavelength $\lambda = 1.55\mu m$. These parameters are chosen in accordance with the paper [3]. The critical gap width $h_c = 5nm$. The HPP-to-CGD crossover point: $d^* \approx 17\mu m$ for $h = 2nm$.

There is a significant difference between the dependence of the effective index n_{CGD} on the gap thickness h for the cases of low and high index dielectric, see Fig. 2. For relatively low refractive index of dielectric, $\varepsilon_d < |\varepsilon_m|$, there exists surface plasmon-polariton mode when the gap is absent, $h = 0$. It has effective index $n_{md} = \sqrt{\varepsilon_m \varepsilon_d / (\varepsilon_d + \varepsilon_m)}$. Then the effective index of the fundamental CGD-mode is bounded, $\sqrt{\varepsilon_d} < n_{CGD} < n_{md}$. Just the case was considered in the papers [5] and [3]. Otherwise when permittivity of dielectric is relatively high

$$\varepsilon_d > |\varepsilon_m| > \varepsilon_g, \tag{3}$$

the effective index n_{CGD} unlimitedly diverges as the gap thickness tends to zero, $h \ll \lambda / \sqrt{\varepsilon_d}$:

$$n_{CGD} \approx \frac{1}{2kh} \ln \frac{(\varepsilon_d - \varepsilon_g)(\varepsilon_m - \varepsilon_g)}{(\varepsilon_d + \varepsilon_g)(\varepsilon_m + \varepsilon_g)}. \tag{4}$$

This leads to extremely strong light confinement in a transparent dielectric gap layer located between the high-index dielectric and the conductor. The actual degree of localization is restricted only by additional factors, such as increasing Ohmic losses in the metal, spatial dispersion and atomic structure of the materials. In this respect the properties of the conductor-gap-dielectric plasmonic mode similar to that of the gap plasmon polaritons in a conductor-gap-conductor structure [8, 9]. This feature is the principle behind our idea: in practice one should choose the metal of the absolute permittivity less than the permittivity of the cylinder and place cylinder at distance $h < h_c$ from the metal plane. When such metal is involved the effective index of the HPP mode can be significantly greater than effective index of electromagnetic field in bulk material of the cylinder even for very small diameters of the cylinder. Note, that to calculate group velocity v_g and chromatic dispersion for the mode using the formula (4), one should know the dispersion laws for permittivities ε_m and ε_d. For thin gap $h \ll h_c$, the group velocity scales as $v_g / c \propto h / \lambda$. Thus divergence of the CGD-mode effective index with the gap width decreasing leads to strong reduction of the group velocity.

There is reverse side of the strong localization which is small propagation distance. It was shown in paper [3] that the strongest localization of the HPP-mode corresponds to the lowest propagation length. It is common place of waveguides which use metal as a constructive component. Let us consider limit when the gap index is low, so $\varepsilon_g \ll |\varepsilon_m|$. For the case

$$n_{\text{CGD}} \approx \frac{1}{kh|\varepsilon_m|} \left(1 - \frac{|\varepsilon_m|}{\varepsilon_d} + i \frac{\varepsilon_m''}{|\varepsilon_m|} \right), \tag{5}$$

where ε_m'' is the imaginary part of the metal permittivity. It follows from Eq. (5), that the localization radius is of the order of $h|\varepsilon_m|$ in the limit $h \ll h_c$. Note, that our approach allows to squeeze the mode at arbitrary frequency into any subwavelength scale simply by tuning the gap width in accordance with (4). Hence, our waveguide design breaks connection between mode localization and the carrying frequency of the mode. In particular, the approach may be interesting for design waveguides at THz frequencies [10, 11]. The propagation length $\ell \sim h|\varepsilon_m|/|tg|$ i.e. reduces with the mode size reduction. To keep the propagation length acceptable for practical implementation at fixed degree of localization one should minimize loss tangent tg. Thus, a prospecting like [12] is needed to propose the optimal choice of materials for our approach (3).

3. Semi-analytical description and numerical results

In the section, we present the semi-analytical approach to the propagation of the HPP-mode and discuss the numerical results. It follows from Maxwell's equations that the electromagnetic field of guiding mode can be fully described by z-components of the electric and the magnetic fields, E_z and B_z [13]. These fields satisfy the following two-dimensional Helmholtz differential equation inside the homogeneous areas where permittivity is constant:

$$\Delta^\perp \left\{ \begin{array}{c} E_z \\ H_z \end{array} \right\} - (\beta^2 - \varepsilon k^2) \left\{ \begin{array}{c} E_z \\ H_z \end{array} \right\} = 0, \tag{6}$$

where $\Delta^\perp = \partial_x^2 + \partial_y^2$ and $k = \omega/c$ is the free space wavenumber. The boundary conditions on the both interfaces are continuity of components E_z, H_z, εE_ξ and H_ξ, where ξ-component of a vector is its normal component.

Our semi-analytical method is based on the representation of the hybrid waveguide as an integration of the dielectric fiber and plane plasmonic waveguide. We express the electromagnetic field of the HPP-mode as a linear combination of cylindrical modes around the fiber and evanescent plane waves above the metal screen. Boundary conditions provide the system of linear equations on the expansion coefficients. Such an approach leads to highly efficient method of numerical solving a difficult boundary-value problems that describe the propagation of waves in a complex systems [14, 15]. The scheme is developed in detail in Appendix A.

To verify our semi-analytical method, in Fig. 3 we present the dependence of the effective index of the fundamental hybrid mode on the cylinder diameter d for a range of the gap widths h in the case of telecommunication wavelength when $\varepsilon_g < \varepsilon_d < |\varepsilon_m|$. These dispersion curves are obtained from our numerical procedure and show a good agreement with the results obtained in [3] by using finite-element package FEMLab from COMSOL.

In accordance with general argumentation given in Section 2 we next present two sets of plots. Fig. 4(a) corresponds to the case of fiber with comparatively low refractive index, $\varepsilon_d < |\varepsilon_m|$, the parameters of the waveguide are taken accordingly to experimental work [16]. Fig. 4(b) corresponds to opposite limit, when $\varepsilon_d > |\varepsilon_m|$. Parameters of these two plots differ only for metal permittivity ε_m, the value $\varepsilon_m = -4$ is chosen for Fig. 4(b). Here, we do not concretize the material of the metal screen, our goal is just to demonstrate the qualitative difference of the guiding mode properties for the case (3).
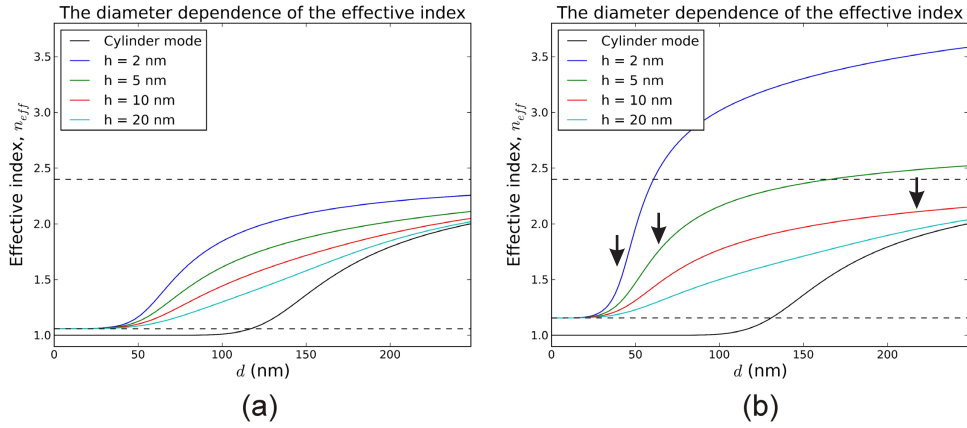
Fig. 4. Effective refractive index of the fundamental hybrid mode versus cylinder diameter d (coloured lines) compared with those of single fiber (black solid line) and SPP mode (lower black broken line). The upper black broken line corresponds to the refractive index of the cylinder. (a) The dielectric constants of the cylinder, dielectric and metal are $\varepsilon_d = 5.76$, $\varepsilon_g = 1$ and $\varepsilon_m = -9.2$ respectively at wavelength $\lambda = 0.49\mu m$. These parameters are chosen in accordance with the paper [16]. The critical gap width $h_c = 7nm$. The HPP-to-CGD crossover points are: $d^* \approx 310nm$ for $h = 2nm$, $d^* \approx 875nm$ for $h = 5nm$. (b) The dielectric constants of the cylinder, dielectric and metal are $\varepsilon_d = 5.76$, $\varepsilon_g = 1$ and $\varepsilon_m = -4$ respectively at wavelength $\lambda = 0.49\mu m$. The critical gap width $h_c = 13,4nm$. The HPP-to-CGD crossover points (black arrows) are: $d^* \approx 40nm$ for $h = 2nm$, $d^* \approx 65nm$ for $h = 5nm$, $d^* \approx 220nm$ for $h = 10nm$.

Presented results indicate that when fiber diameter d is decreased, the HPP-mode loses confinement along the metal and eventually (at $d = 0$) becomes a surface plasmon-polariton mode of the flat metal-vacuum interface. Herewith the effective index of the HPP-mode monotonically decreases to that of this SPP-mode. Thus all dispersion curves have the same asymptotic $n_{eff} \to n_{mg} = \sqrt{\varepsilon_m \varepsilon_g/(\varepsilon_m + \varepsilon_g)}$ at small d. Two different behavior are possible at the opposite limit of large diameter. As the diameter $d \to \infty$, the HPP-mode can asymptotically tend either fundamental single fiber mode or the fundamental mode of the planar three-layer system, the choice depends on the gap width h. If the gap thickness h is below than h_c (Eq. (2)) the HPP-mode approaches the CGD-mode with the diameter increasing. In the case the crossover between the asymptotics occurs at d^* (black arrows at Fig. 4(b)) which is determined as

$$d^* \approx \frac{1}{4(n_{CGD}^2 - \varepsilon_d)hk^2}. \tag{7}$$

For $h > h_c$ the HPP-mode becomes the cylinder-like in the limit of the large diameter. In the case the critical diameter d_0 corresponding to the transition between small-diameter and large-diameter asymptotics is defined by the equation $n_{SF}(d_0) = n_{mg}$, where $n_{SF}(d)$ is the diameter dependence of the effective index of the single fiber fundamental mode. If the condition $\sqrt{\varepsilon_d}kd \ll 1$ is valid one can derive that the localization of this mode is exponentially small, $n_{SF} = \sqrt{\varepsilon_g} + \kappa_g^2/(2\sqrt{\varepsilon_g}k^2)$, where

$$\kappa_g^2/k^2 \approx \frac{16e^{-2\gamma+1}}{(kd)^2} \exp\left\{-\frac{8(\varepsilon_d + \varepsilon_g)}{\varepsilon_g(\varepsilon_d - \varepsilon_g)(kd)^2}\right\} \ll 1, \tag{8}$$

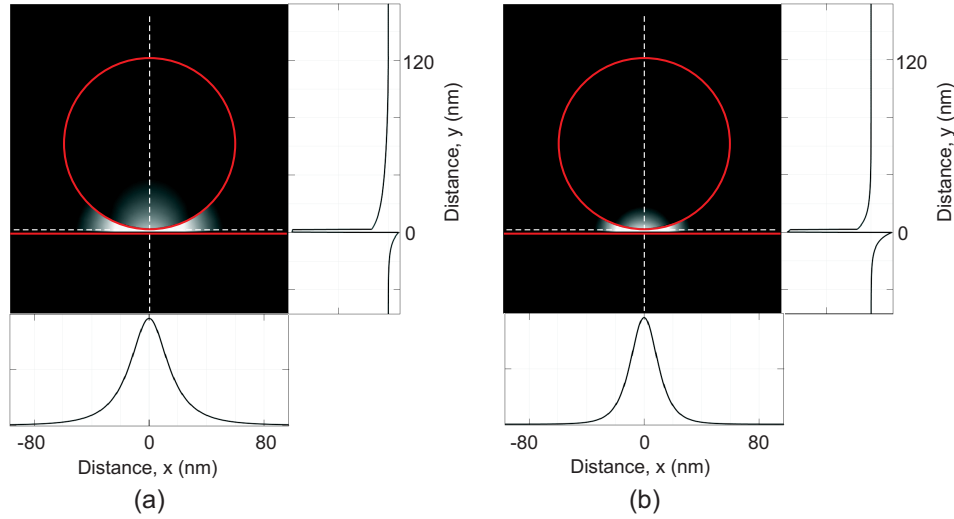and $\gamma = 0.5772...$ is Euler-Mascheroni constant.

Fig. 5. Spatial distribution of the time-average z-component of the Poynting vector $S_z(x,y)$ for the fundamental HPP-mode. The diameter of the cylinder is $d = 120nm$ and the gap width is $h = 2nm$. The dielectric constants of the cylinder and dielectric are $\varepsilon_d = 5.76$ and $\varepsilon_g = 1$ respectively at wavelength $\lambda = 0.49\mu m$. (a) The dielectric permittivity of the metal is $\varepsilon_m = -9.2$, (b) $\varepsilon_m = -4$.

Let us suppose the effective index n_{CGD} of the CGD-mode not to be significantly above that of bulk plane wave in the fiber medium, $\sqrt{\varepsilon_d}$. For example, this assumption is true at the conventional plasmonic condition when the absolute value of metal permittivity is sufficiently greater than the dielectric permittivity, $|\varepsilon_m| > \varepsilon_d$. Just the case is realised at Fig. 3 and Fig. 4(a). Then the field penetration depth into the upper dielectric is quite large as well as the HPP-to-CGD crossover diameter $d^* > \lambda$, so the CGD-mode does not provide the strong confinement. Therefore there are no advantages of CGD-like limit in the case from the view of HPP-mode confinement. For a given frequency and gap width the choice with the strongest coupling of the fiber mode and the surface plasmon polariton mode, corresponding to $d = d_0$, provides the strongest localization of the field within nanogap due to the great contrast of permittivities [3]. The Fig. 5(b) visualises the spatial distribution of the time-average Poynting vector for the optimum value of the diameter and $h = 2nm$. At the same time significant part of energy is transferred inside the fiber, thus the waveguide mode confinement is achieved largely due to the boundedness of the high-permittivity dielectric part of the waveguide. Once the diameter of the fiber is optimum and the gap width is small enough the advantages of the hybrid architecture are used completely: cross section size of the system can be much less than the wavelength and mode confinement is much stronger than for uncoupled single fiber or flat metal-dielectric interface. To achieve further increase of the HPP-mode confinement the fiber with higher dielectric constant should be used.

Next let us assume that effective index of the CGD-mode is significantly larger than the refractive index of the fiber medium. This can be achieved by diminishing the gap thickness in the case $|\varepsilon_m| < \varepsilon_d$ that corresponds to the Fig. 4(b). Then the CGD-mode has strong confinement so the crossover diameter can be decreased to deep subwavelength scale, $d^* \ll \lambda$, by tuning the gap width. Therefore the attractive CGD-like asymptotic can be achieved by HPP-mode with very small diameter of cylinder providing the wished structure of the mode with the strong transversal localization in two dimensions within the gap region and exponential decaying into

The diameter dependence of the propogation distance

Propogation distance $/\lambda$
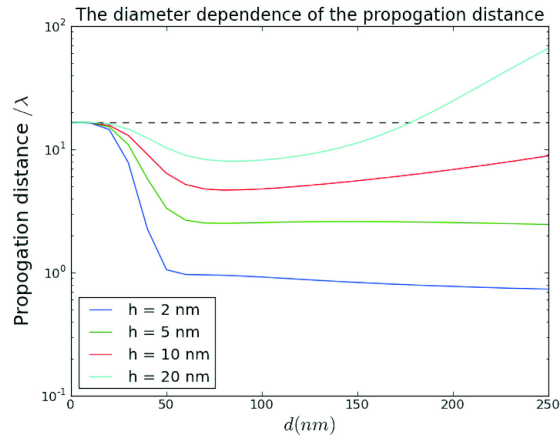
$d(nm)$

h = 2 nm
h = 5 nm
h = 10 nm
h = 20 nm

Fig. 6. The fundamental HPP-mode's propagation distance in dependence on cylinder diameter (coloured lines) compared with propagation distance of pure SPP-mode at metal-dielectric interface (black broken line). The dielectric constants of the cylinder, dielectric and metal are $\varepsilon_d = 5.76$, $\varepsilon_g = 1$ and $\varepsilon_m = -4 + 0.1i$ respectively at wavelength $\lambda = 0.49\mu m$.

the cylinder. The example of the spatial distribution of the time-average Poynting vector is represented in Fig. 5(b). Note that in the case the top part of the fiber cross section is at distances much larger than $1/\kappa_d$ from the gap and its particular shape does not play role any more. As it was mentioned above the propagation distance decreases with the gap width decreasing, see Eq. (5). We present the results of simulation performed by using the COMSOL commercial software package in Fig. 6. The ultra-small mode confinement leads to storage of the large portion of the electromagnetic energy within dissipative metal region. Thus the stronger localization corresponds to the shorter HPP-mode's propagation length.

4. Conclusion

In the paper we have proposed the novel approach for hybrid plasmonic waveguide design providing wide opportunities for HPP-mode property controlling. When the absolute permittivity of the metal is less than that of the dielectric the hybrid effective index is unlimitedly diverges (Eq. (4)) with the gap width decreasing. High effective index provides strong confinement of the electromagnetic field in two dimensions within the nanometer-scale gap region. Thus the mode size can be simply controlled by tuning the waveguide' geometry at fixed frequency and materials constituting the waveguide. The advantages of the case $|\varepsilon_m| < \varepsilon_d$ are confirmed by both qualitative analysis within planar three-layer model and rigorous semi-analytical method describing the HPP-mode propagation in general. The propagation distance of hybrid mode reduces with the mode size reduction. To achieve long-range propagation at fixed degree of localization one should minimize loss tangent $tg = |\varepsilon_m''/\varepsilon_m'|$ of the metal. It should be noted that simultaneous satisfying of both conditions $|\varepsilon_m| < \varepsilon_d$ and $tg \ll 1$ at optical and near infrared frequencies is a challenging task. Thus implementation of the waveguide loss compensation techniques would be required to use such hybrid waveguide as a component of the miniaturized photonic circuits. Another potential application of our waveguide design lies in study field of the resonant plasmons. The resonance condition for a surface plasmon-polariton at a planar metal-dielectric interface is the fine-tuning of the permittivities, $-(\varepsilon_m + \varepsilon_d) \ll \varepsilon_d$ [17]. Thus for particular metal the resonance can be achieved only in a narrow spectral range. While
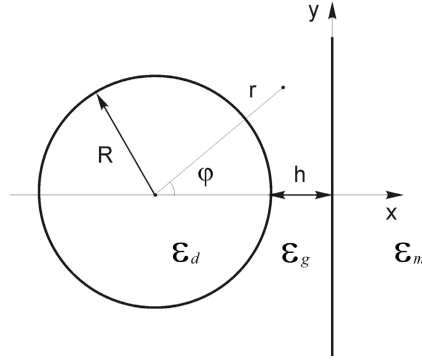
Fig. 7. Reference system.

resonant increasing of the CGD-mode effective index requires only the geometrical condition $h \ll \lambda$. Thus for the conductor-gap-dielectric structure the resonance of plasmonic mode can be attained by gap width decreasing at any frequency as long as the condition $|\varepsilon_m| < \varepsilon_d$ is valid.

A. Numerical method

The theoretical description of the hybrid waveguide is inhibited by its complex geometry. In general we should chose such system of coordinates where the surfaces of the waveguide are the isolines and Helmholtz equation can be solved by separation of variables. The hybrid geometry corresponds to the so called bipolar coordinates based on two sets of orthogonal circles. In this coordinate system the Helmholtz equation has quite complicated form and accordingly the set of eigen functions cannot be found analytically. However the unknown hybrid eigen functions can be expressed in terms of known solutions of the Helmholtz equation in other coordinate systems. It is convenient to represent the total electromagnetic field of HPP-mode as the superposition of the all modes of single fiber(cylindrical functions) and all SPP modes(evanescent plane waves) with some unknown coefficients of expansion.

We chose the Cartesian system of coordinates with origin at axis of the cylinder which is z-axis (Fig. 7). Supposing the structure of the fundamental hybrid mode to be symmetric with respect to x-axis we can describe the longitudinal component of the electric field as

$$
\begin{cases}
E_z^{(d)} = \sum_{n=0}^{\infty} a_n^{E} J_n(\chi_d r) \cos n\varphi \\
E_z^{(g)} = \sum_{n=0}^{\infty} b_n^{E} K_n(\kappa_g r) \cos n\varphi + \\
\quad + \int_0^{\infty} c_q^{E} \exp(Q\kappa_g(x-D)) \cos q\kappa_g y \, dq \\
E_z^{(m)} = \int_0^{\infty} d_q^{E} \exp(-Q\kappa_m(x-D)) \cos q\kappa_m y \, dq
\end{cases}
\tag{9}
$$

and z-components of the magnetic field as

$$
\begin{cases}
H_z^{(d)} = \sum_{n=0}^{\infty} a_n^{H} J_n(\chi_d r) \sin n\varphi \\
H_z^{(g)} = \sum_{n=0}^{\infty} b_n^{H} K_n(\kappa_g r) \sin n\varphi + \\
\quad + \int_0^{\infty} c_q^{H} \exp(Q\kappa_g(x-D)) \sin q\kappa_g y \, dq \\
H_z^{(m)} = \int_0^{\infty} d_q^{H} \exp(-Q\kappa_m(x-D)) \sin q\kappa_m y \, dq
\end{cases}
\tag{10}
$$

where $Q = \sqrt{1+q^2}$ and $D = d/2 + h$.

To write the corresponding equations, it is convenient to express the field inside dielectric in terms of only plane evanescent waves, when we impose the continuity conditions on the

boundary of the metal, and in terms of angular harmonics, for the cylindrical surface. We solve it by using the evanescent plane wave expansion of modified cylindrical functions and angular harmonic spectrum of the evanescent plane waves [18]

$$K_n(\kappa_g r)\cos n\varphi = \int_0^\infty F_n^{\mathrm{E}}(q)e^{-Q\kappa_g x}\cos q\kappa_g y\,\mathrm{d}q, \tag{11}$$

$$K_n(\kappa_g r)\sin n\varphi = \int_0^\infty F_n^{\mathrm{H}}(q)e^{-Q\kappa_g x}\sin q\kappa_g y\,\mathrm{d}q, \tag{12}$$

$$e^{Q\kappa_g x}\cos q\kappa_g y = \sum_{n=0}^\infty G_n^{\mathrm{E}}\cos n\varphi, \tag{13}$$

$$e^{Q\kappa_g x}\sin q\kappa_g y = \sum_{n=0}^\infty G_n^{\mathrm{H}}\sin n\varphi, \tag{14}$$

where

$$F_n^{\mathrm{E}} = \frac{(Q+q)^n + (Q-q)^n}{2Q}, \tag{15}$$

$$F_n^{\mathrm{H}} = \frac{(Q+q)^n - (Q-q)^n}{2Q}, \tag{16}$$

$$G_n^{\mathrm{E}} = \frac{2-\delta_{0n}}{2}((Q+q)^n + (Q-q)^n)I_n(\kappa_g r), \tag{17}$$

$$G_n^{\mathrm{H}} = ((Q+q)^n - (Q-q)^n)I_n(\kappa_g r). \tag{18}$$

Thus the electromagnetic fields in surrounding medium close to the dielectric waveguide can be written as

$$E_z^{(g)} = \sum_{n=0}^\infty b_n^{\mathrm{E}} K_n(\kappa_g r)\cos n\varphi\ +$$

$$+ \sum_{n=0}^\infty \cos n\varphi \int_0^\infty c_q^{\mathrm{E}} G_n^{\mathrm{E}}(r,q)e^{-Q\kappa_g D}\,\mathrm{d}q,$$

$$H_z^{(g)} = \sum_{n=0}^\infty b_n^{\mathrm{H}} K_n(\kappa_g r)\sin n\varphi\ +$$

$$+ \sum_{n=0}^\infty \sin n\varphi \int_0^\infty c_q^{\mathrm{H}} G_n^{\mathrm{H}}(r,q)e^{-Q\kappa_g D}\,\mathrm{d}q.$$

The corresponding expressions for the fields close to the surface of the metal are

$$E_z^{(g)} = \int_0^\infty \sum_{n=0}^\infty b_n^{\mathrm{E}} F_n^{\mathrm{E}}(q)e^{-Q\kappa_g x}\cos q\kappa_g y\,\mathrm{d}q\ +$$

$$+ \int_0^\infty c_q^{\mathrm{E}} e^{Q\kappa_g(x-D)}\cos q\kappa_g y\,\mathrm{d}q,$$

$$H_z^{(g)} = \int_0^\infty \sum_{n=0}^\infty b_n^{\mathrm{H}} F_n^{\mathrm{H}}(q) e^{-Q\kappa_{\mathrm{g}} x} \sin q\kappa_{\mathrm{g}} y \, \mathrm{d}q \, +$$

$$+ \int_0^\infty c_q^{\mathrm{H}} e^{Q\kappa_{\mathrm{g}}(x-D)} \sin q\kappa_{\mathrm{g}} y \, \mathrm{d}q.$$

It can be easily derived from the Maxwell's equations that for the normal components

$$E_\xi \quad = \quad -\frac{i\beta}{\beta^2 - \varepsilon k^2} \frac{\partial E_z}{\partial \xi} + \frac{ik}{\beta^2 - \varepsilon k^2} \frac{\partial H_z}{\partial \eta}, \tag{19}$$

$$H_\xi \quad = \quad -\varepsilon \frac{ik}{\beta^2 - \varepsilon k^2} \frac{\partial E_z}{\partial \eta} - \frac{i\beta}{\beta^2 - \varepsilon k^2} \frac{\partial H_z}{\partial \xi}, \tag{20}$$

where η is tangent to the interface coordinate in the transversal plane.

The continuity conditions on the metal surface for E_z, B_z, εE_x and εB_x lead to the first system of linear homogeneous equations (SLE) on coefficients b_n^{E}, b_n^{H}, c_q^{E}, c_q^{H}, d_p^{E}, d_p^{H}. The corresponding continuity conditions for E_z, B_z, εE_r and εB_r on the cylindrical surface produce the second SLE on amplitudes a_n^{E}, a_n^{H}, b_n^{E}, b_n^{H}, c_q^{E}, c_q^{H}, which is now integral with respect to c_q^{E}, c_q^{H}. In order to avoid integration of the unknown functions we express the coefficients c_q^{E}, c_q^{H} in the terms of b_n^{E}, b_n^{H} from the first SLE and substitute them into the second SLE. The procedure leads to the infinite system of linear homogeneous algebraic equations for coefficients a_n^{E}, a_n^{H}, b_n^{E}, b_n^{H}. In order to solve the system numerically one should truncate it to a finite size. Then the propagation constant of the fundamental hybrid mode can be determined from the condition of vanishing of the characteristic determinant.

Acknowledgments